Referee 2:

We thank Referee 2 for taking the time to review our manuscript and the valuable feedback. We have corrected the manuscript according to the referee’s comments.

The manuscript by Nussbaumer et al. provides the first HCHO budget calculations across Europe using *in situ* measurements as opposed to evaluating the HCHO budget using model simulations. Additionally, the authors show that HCHO production is dominated primarily by the oxidation of methane, methanol, acetaldehyde, and isoprene during three campaigns (CYPHEX, HOPE, and HUMPPA) representing a coastal, mountain, and forested site, respectively. The HCHO yield from isoprene and fraction of methyl peroxy radicals (CH3O2) forming HCHO were also shown as an alternative method for determining whether a location is NOx or VOC-limited (or in some transition regime).

General comments: While the oxidation of methane, methanol, acetaldehyde, and isoprene are the dominant VOC precursors to HCHO production, care should be taken throughout the manuscript to never imply that only these four chemical species make up the entirety of the HCHO budget. HCHO is commonly used as a VOC tracer and comes from more than simply those four species as the authors showed with the pie chart in Figure 6. As an example, Line 75 is misleading since it states that "HCHO production can be accounted for by the oxidation of methane, methanol, acetaldehyde, and isoprene" which implies 100%. Rather, it should read "...predominantly accounted for..." or some other conditional phrasing.

We agree with the referee and have clarified that the four mentioned VOC precursors do not account for 100%, but rather dominate the HCHO production.

Lines 76 ff.: We are first to present HCHO budget calculations from in-situ measurements across Europe and show that in all three locations HCHO production can be predominantly accounted for by the oxidation of methane, methanol, acetaldehyde and isoprene.

Lines 363 f.: (…) leads to the conclusion that HCHO production can be approximated by OH oxidation of methane, acetaldehyde, isoprene and methanol.

Lines 500 ff.: Very consistently across all sites, we found that formaldehyde loss can be predominantly accounted for by the production via OH oxidation of methane, acetaldehyde, isoprene and methanol.

The manuscript fits well within the scope of ACP and provides a good, detailed analysis of uncertainty. I recommend publication after attention to the previous general comment and the following specific comments/technical corrections.

We thank the referee for this positive feedback and the recommendation for publication.

Specific Comments:

- For the reader, explicitly define somewhere in the text what is meant by "atmospheric variability" (i.e., what factors control this uncertainty)

We have added text to explain the term “atmospheric variability”.

Lines 249 ff.: Besides the uncertainty resulting from the calculation, an additional uncertainty arises from the atmospheric variability which describes ambient, instrumentally independent variations of the considered trace gases and parameters caused by for example atmospheric turbulence.

- Whenever mentioning the detection limit of an instrument (for instance, in Section 2.3.1), the integration time necessary to achieve that detection limit should be mentioned.

Unless otherwise stated, the detection limits refer to the time resolution which is shown in Table S3 of the Supplement. We have added text for clarification.

Line 213: All stated detection limits refer to the time resolution shown in Table S3 of the Supplement.

Line 264 f.: CH3OH was measured via ColdTrap PTR-MS with a detection limit of around 50 pptv (integration time of 5 mins).

- Figure 1: There is space above (or below) the HCHO precursors to write the actual chemical name for each of the chemical formulas (i.e., acetone, MHP, etc.)

We have changed the Figure according to the referee’s suggestion.

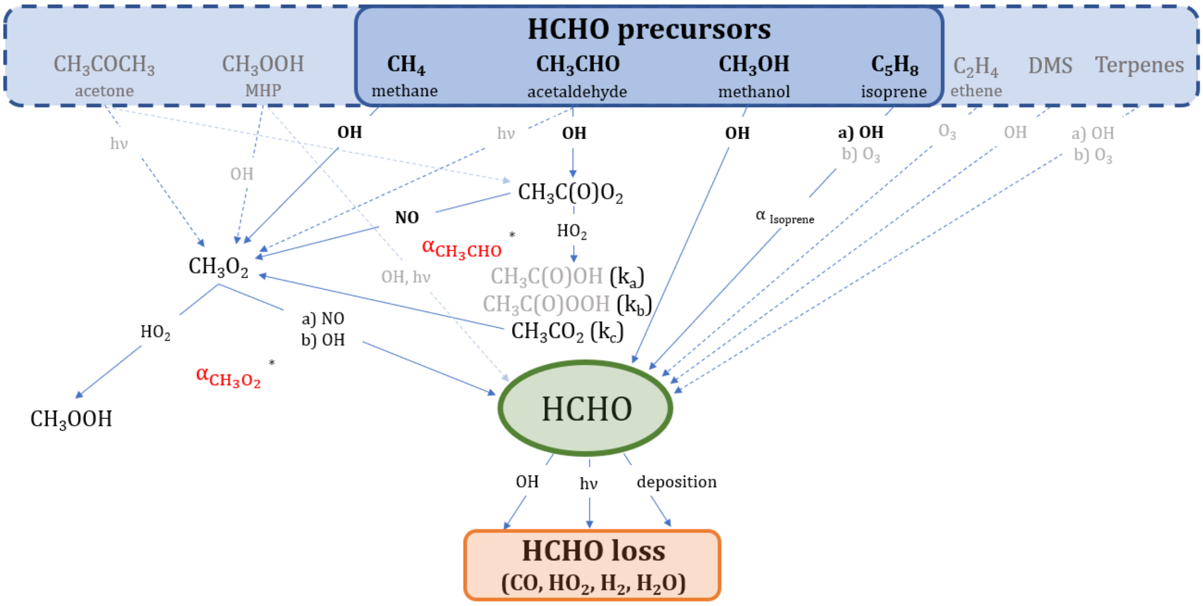

$$^{*}\alpha_{CH_3CHO} = \frac{k_{CH_3C(O)O_2+NO} \times [NO] + k_c \times [HO_2]}{k_{CH_3C(O)O_2+NO} \times [NO] + k_a \times [HO_2] + k_b \times [HO_2] + k_c \times [HO_2]}$$

$$^{*}\alpha_{CH_3O_2} = \frac{k_{CH_3O_2+NO} \times [NO] + k_{CH_3O_2+OH} \times [OH]}{k_{CH_3O_2+NO} \times [NO] + k_{CH_3O_2+OH} \times [OH] + k_{CH_3O_2+HO_2} \times [HO_2]}$$

- Line 197: The determination of the acetaldehyde and formaldehyde photolysis frequencies are from a parameterization using IUPAC quantum yield data and measurements of j(NO2) and j(O1D). This parameterization should be explicitly shown in the SI for the reader.

We now present the details on the parameterization in Table S2 and Equation (S1) of the Supplement. We additionally show an example for the performance of the parameterization in Figure S2 of the Supplement. We have added text in the manuscript for clarification.

Lines 204 ff.: The photolysis frequencies for acetaldehyde j(CH3CHO) and formaldehyde j(HCHO) were determined via parameterizations based on j(NO2) and j(O1D) according to Equation (S1) with the coefficients presented in Table S2 of the Supplement. The latter were derived from least-squares fits to photolysis frequencies from a large set of spectroradiometer measurements at Jülich, Germany (Bohn et al., 2008) under all weather conditions and were originally derived for the HUMPPA campaign. In this work more recent quantum yields for the HCHO photolysis as recommended by IUPAC (2013) were used with an estimated uncertainty of 20%. An example for the performance of the parameterization is shown in Figure S2 of the Supplement.

Figure S2: Correlations of measured j(HCHO) (molecular plus radical channel) with (a) j(O1D) and (b) j(NO2) from spectroradiometer measurements. The correlation of measured and parameterized j(HCHO) according to Equation (S1) is shown in panel (c). Only one out of ten data points from the original data set is shown for clarity.

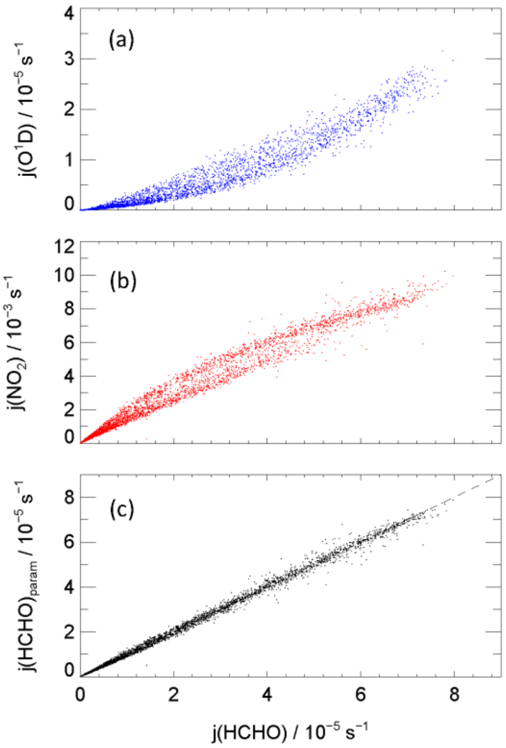

Table S2: Coefficients for the calculation of j(HCHO) and j(CH3CHO) according to Equation (S1).

species	a_1	a_2 [s]	b_1	b_2 [s]
HCHO	1.719	-1.768×10^{4}	4.701×10^{-3}	-3.471×10^{-2}
CH_3CHO	1.516×10^{-1}	-8.970×10^{2}	4.567×10^{-5}	1.711×10^{-3}

Equation (S1):

$$j(species)_{parameter} = a_1 \times j(O^1D) + a_2 \times (j(O^1D))^2 + b_1 \times j(NO_2) + b_2 \times (j(NO_2))^2$$

- Figure 4: At least for the example shown, it is odd that points were selected when the HCHO mixing ratio was still increasing and were included in the fit. In this particular case, the slope would be underestimated and the deposition velocity would be biased. What motivated the decision to always select points between 21:00 - 01:30 UTC as opposed to looking at the underlying nighttime HCHO mixing ratio data over several hours?

We intended to find a reproducible nighttime period with decreasing HCHO concentrations which could be applied to all nights. Choosing the data between 21:00 and 01:30 UTC for HOPE and between 00:00 and 04:30 UTC for HUMPPA is the best compromise regarding all considered nights. However, when individually choosing the time period for each night, the deposition velocity for HOPE rises to 0.94cm-1 during the day and 0.47cm-1 during the night (compared to 0.40 cm-1 and 0.20 cm-1 for a constant time period). For HUMPPA, we get 0.87cm-1 during the day and 0.43cm-1 during the night (compared to 0.72 cm-1 and 0.36 cm-1 for a constant time period). We have updated our calculations and the Figures using the new velocities according to the referee's suggestion. There are no significant changes to the results discussed in the manuscript.

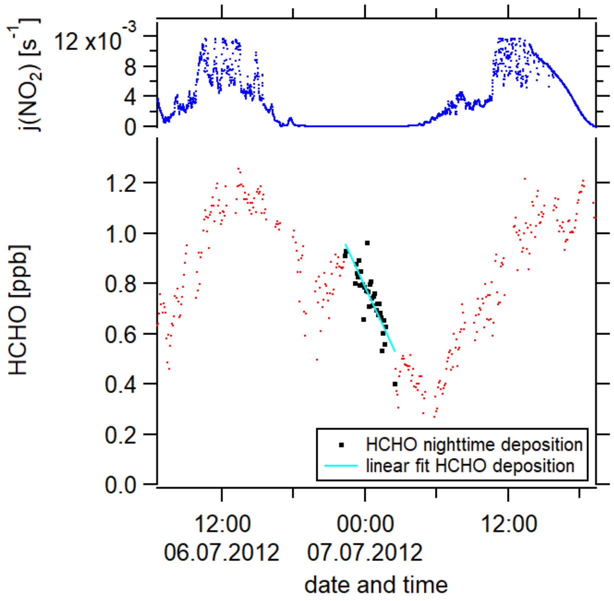

Lines 237 f.: (…) the nighttime deposition velocity according to Equation (11) which gives vd(day)=0.94cm s-1 and vd(night)=0.47cm s-1.

Lines 274 f.: The deposition velocity was determined in analogy to the HOPE campaign based on the nighttime HCHO loss on the basis of 14 nights and was 0.85cm s-1 during the day and 0.43cm s-1 during the night.

- Lines 395-396: Please create pie charts for HOPE and HUMPPA (as done for CYPHEX) since this readily shows the contributions of the four dominant precursors as well as the other reactions included in your chemical mechanism. Could either place resulting figure in main text or SI.

The pie chart we have created for CYPHEX is based on a balance to the HCHO loss which worked well because the summed production terms are smaller compared to the loss terms. However, for HUMPPA and HOPE, we find that the HCHO production term approximated by oxidation of the four mentioned VOC precursors is slightly higher compared to the overall loss term. We suggest this effect to be the result of a transport effect from areas with lower HCHO concentrations. We show the pie charts based on the summed HCHO production terms in Figure S10 of the Supplement and refer to it in the main text.

Lines 414 f.: We show a pie chart representing the contribution of the single HCHO production terms during HOPE in Figure S10a of the Supplement.

Lines 424: Figure S10b shows the share of the individual HCHO production terms during HUMPPA.

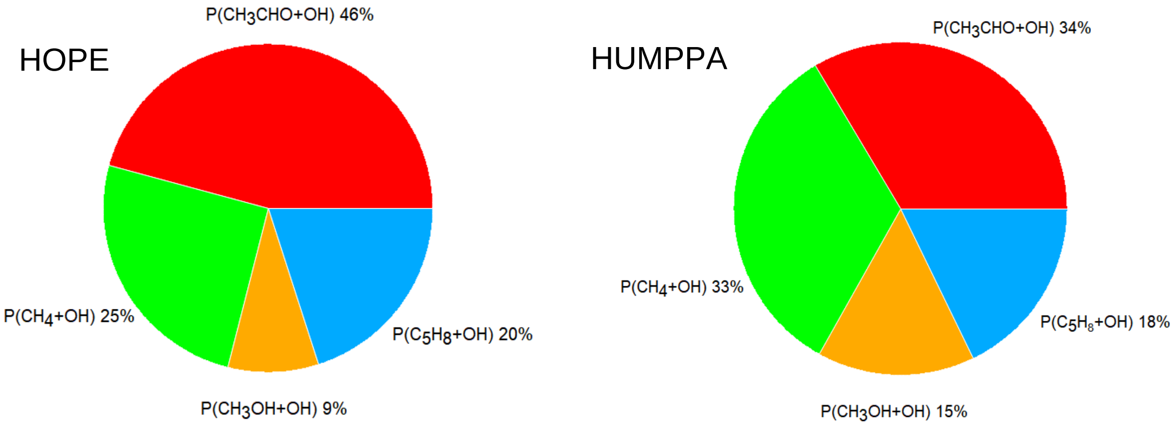

Line 475: Explicitly state that specialized instrumentation is still required (particularly for OH and HO2) for these alternative methods of determining the chemical regime.

We have added text to indicate that the measurement of NO, OH and HO2 needs particular instruments.

Lines 494 ff.: Although specialized instrumentation is still necessary to measure NO, OH and HO2, these methods to determine the dominant chemical regime only require the knowledge of a small number of trace gas concentrations and the ambient temperature.

Technical Corrections:

Throughout text: Formatting for d[HCHO]/dt is inconsistent (for example, line 260 and 275)

We have unified the format to $\frac{d[HCHO]}{dt}$.

Line 404: Misspelling of acetaldehyde

Thank you, we have corrected this.

Figure S7A: Please clarify whether the data is from CYPHEX or HUMPPA

Thanks for pointing this out, these are the data for HUMPPA. We have corrected the Figure title accordingly.

Figure S11: Diurnal HCHO production and loss during HUMPPA (…)

Figures: Font size on axes should be increased since the axes are hard to read when printed

We have increased the font size of all axis labels.